

Numerical Investigation of Heat Transfer Enhancement for a Perforated Fin in Natural Convection

Mohamad I. Al-Widyan*, Amjad Al-Shaarawi**

*(On Sabbatical Leave from Jordan University of Science and Technology, PO Box 3030, Irbid 22110,
Jordan. Permanent e-mail: widyan@just.edu.jo) in the

Mechanical Engineering Department
King Faisal University, PO Box 380, Al-Ahsa 31982, Saudi Arabia

** (Mechanical Engineering program - Clean Combustion Research Center
4700 King Abdullah University of Science and Technology
Thuwal Saudi Arabia

ABSTRACT

This work considered a rectangular fin with a uniform cross section embedded with circular perforations attached to a surface at a constant temperature. The perforated fin was analyzed under natural convection using FLUENT ANSYS for heat transfer enhancement relative to its solid counterpart considering different levels of Grashof numbers and two geometric parameters: spacing between holes, s_x , and hole diameter, D . It was found that, over the ranges considered, heat transfer from the perforated fin increased with Grashof number. In addition, heat transfer increased as the spacing between holes decreased. As for the hole diameter, almost all cases showed an increase in heat transfer with diameter except for the case of high Grashof number (1×10^6) and high spacing ratio, ϵ , where a maximum value of heat transfer enhancement is reached then started to decrease again with the diameter calling for further investigation that includes the fin thickness.

Keywords- FLUENT ANSYS, Geometric parameters, Heat transfer enhancement, Natural convection, Numerical solution, Perforated fin

1. Introduction

In a countless number of applications, the production of excess heat in system components is inevitable. If not adequately removed, this excess heat may have detrimental consequences on the operation and functioning of those components. In many such applications, it is not possible or practicable to introduce cooling liquid fluids or even utilize forced gas convection where needed. It is such cases when natural convection, normally with air as the cooling medium, comes into play as the only viable cooling option. Natural convection finds very wide applications in a host of heat exchange processes ranging from cooling of tiny electronic components [1] to cooling of fuel elements in nuclear reactors.

The utilization of natural convection in cooling processes is almost always associated with the use of extended surfaces, also known as fins, for the sake of enhancement of the process by increasing the heat transfer area. This is especially true, and necessary, when gases are utilized as cooling media, which is dominantly the case. The reason is that gases possess convection coefficients that are an order of magnitude less than those of liquids [1].

Generally speaking, heat transfer between a surface and a fluid can be enhanced either actively or passively [2] where active methods require an external power source while passive methods don't. Fins represent the prime example on passive methods. However, for fins to be effective, they must be carefully designed and accurately incorporated, which requires full understanding of the aspects accompanying the use of fins. It is well-known that fins come in various types but the rectangular straight fin is perhaps the most common design mainly due to its fabrication simplicity. One major aspect of fin design involves fin optimization that entails either minimizing volume or mass for a given heat dissipation rate or maximizing heat dissipation rate for a given volume or mass as reported in [3] and [4]. Other desirable effects of fin optimization include weight reduction and material costs [5].

A vast volume of literature does exist on using fins for heat transfer enhancement and a great deal of analytical and experimental work has been conducted on the various facets of using fins in heat exchange

processes. A closely related and relevant facet to this study is when surface modifications are introduced to the rectangular basic shape for a single fin or an array. It is well-known that such modifications including employing perforations in the fin surface represent a proven tool of heat transfer enhancement [6]. Moreover, perforated fins provide potentially better performing fins as they offer less flow resistance compared to the solid counterpart [7].

Although sufficient and accurate correlations exist for heat transfer calculations for the solid rectangular and other shapes of fins, perforated fins, to the best of the authors' knowledge as based on an extensive literature search, have not been adequately investigated when embedded with perforations in the sense introduced in this study whether it is over the fin perforated surfaces or, and especially, within the perforations themselves. Previous related studies considered similar fins but utilized rough approximations for heat transfer calculations especially when it came to inside the holes [8].

This study considers a single straight rectangular fin embedded with vertical circular perforations that are cut through the fin's body. The fin is attached to a vertical surface at a uniform temperature T_s and operates under natural convection conditions. The study aims at examining the potential enhancement of heat transfer rate due to perforations especially as affected by fin geometric as well as flow parameters using the FLUENT ANSYS software package. As such, the study may well serve as an important first step towards formulating reliable heat transfer correlations applicable to perforated surfaces as well as within perforations.

2. Materials and Methods

As indicated earlier, this study considers a single straight rectangular fin with a uniform thermal conductivity, uniform cross section with length L , thickness of $0.1L$, and is infinitely wide. The fin is perforated with columns of circular holes along the fin length and repeated across the fin width. Each column consists of three identical circular perforations. Each perforation (hole) has a diameter D and is cut vertically through the fin's body (thickness). The columns of holes are separated from one another by a distance S_x in the direction perpendicular to the fin length. In the same column, holes are uniformly distributed in the direction of L and are separated by a distance $S_y = L/4$. The fin is attached to a vertical surface at a fixed temperature T_s and operates under natural convection conditions where the adjoining fluid is assumed to have constant properties with a uniform temperature, T_∞ . A schematic diagram of the fin considered in this study is shown in Fig. 1.

The fin geometry was described by a three-dimensional mesh with 200,000 to 400,000 control volumes depending on fin dimensions. A sample of the mesh utilized is depicted in Fig. 2.

The parameters studied are Grashof number, Gr , and two geometry parameters at a constant Prandtl number, Pr . Grashof number, Gr , and Prandtl number, Pr , are given by:

$$Gr = \frac{g\beta(T_s - T_\infty)L^3}{\nu^2} = \frac{g\beta(T_s - T_\infty)L^3\rho^2}{\mu^2} \quad (1)$$

$$Pr = \frac{c_p\mu}{k} = 0.7 \text{ (fixed at 0.7 for air in this study)} \quad (2)$$

where: g = gravitational acceleration

β = expansion coefficient of the fluid

T_s = surface temperature

T_∞ = Temperature at the fluid boundaries

μ = Dynamic viscosity

ρ = Density

L = Characteristic length (defined in "geometry" file)

k = Thermal conductivity

As far as the geometry parameters are concerned, the study considered the effect of variations in fin length, L , hole spacing, S_x , and hole diameter, D by utilizing two dimensionless parameters, specifically, dimensionless hole spacing, ϵ , and dimensionless hole diameter, δ , defined as follows:

$$\epsilon = \frac{S_x}{D} \quad \text{and} \quad \delta = \frac{D}{L} \quad (3)$$

These two geometric parameters were investigated at three levels each; ϵ took the values of 5, 7.5, and 10, while δ took the values 0.05, 0.10, and 0.15. In such cases, the ideal situation entails sampling the whole infinite spectrum, which is clearly not possible. Thus, the three levels indicated above were chosen randomly but were subject to a range that was considered reasonably practical in terms of size. In addition, as far as δ is concerned, it may be noted that the values were chosen relative to the fin thickness in such a way that one diameter was smaller than, one was equal to, and the third was larger than the fin thickness. This arrangement resulted in nine different geometries. At the boundaries, symmetry planes were placed at the center of the holes and at the mid distance between each column of holes. Atmospheric conditions were assumed at the far field at the lower, top, and front planes.

Gas properties were assumed constant and were chosen in such a way that three particular levels of Grashof number, Gr, specifically, 10^4 , 10^5 , and 10^6 , would result. As such, the total number of different cases considered in this study was 27 test cases which is the result of nine geometries under three levels of Grashof number. Gas properties were also chosen to have Prandtl number, Pr, fixed at 0.7, representing air. In order to account for the buoyancy effect, Boussinesq model was used and the following additional source term was added to the momentum equation:

$$Q = g \beta (T_{\infty} - T) \quad (4)$$

For each of the twenty seven cases considered in this work, the continuity, momentum (including the Boussinesq buoyancy term), and energy equations were solved simultaneously using FLUENT ANSYS software package with convergence criterion set, respectively, at 10^{-5} , 10^{-5} , and 10^{-6} . For all equations, the second order upwind discretization scheme was used.

The enhancement of heat transfer due to the introduction of perforations was assessed by calculating the ratio of the Nusselt number for the perforated fin, Nu_p , and its solid counterpart, that is, Nu_p/Nu_s . On the other hand, the temperature, velocity, and vorticity contours in and about the perforated fin were determined simply from the solution of the three equations mentioned above. For representation (plotting) purposes, the temperature, velocity, and vorticity were all expressed in dimensionless parameters as t^* , u^* , and ω^* , respectively. These groups are given by:

$$t^* = \frac{T - T_{\infty}}{T_s - T_{\infty}} \quad (5)$$

$$u^* = \frac{u}{u_{\text{reference}}} = \frac{u}{L/\left(\frac{L^2}{\nu}\right)} = \frac{u}{\nu/L} \quad (6)$$

$$\omega^* = \frac{\omega}{\omega_{\text{reference}}} = \frac{\omega}{1/\left(\frac{L^2}{\nu}\right)} = \frac{\omega}{\nu/L^2} \quad (7)$$

3. Results and Discussion

It was elected to express heat transfer enhancement as the ratio of the Nusselt number for the perforated fin, Nu_p , to the Nusselt number of the solid counterpart, Nu_s , that is, Nu_p/Nu_s . This ratio was plotted versus Gr with δ as a parameter at three different levels of ϵ , namely, for ϵ equals 5, 7.5, and 10 as shown in Fig. 3 through 5. For all the cases considered, heat transfer enhancement increased as Grashof number, Gr, increased. It is established that as Grashof number increases, the effect of buoyancy forces that push the gas through the holes becomes more dominant than viscous forces that prevent gas from moving through the narrow space in the holes.

In an attempt to make the outcomes even more apparent, the ratio Nu_p/Nu_s was also plotted versus ϵ at three levels of Gr, namely, for Gr equals 10^4 , 10^5 , and 10^6 as depicted in Fig. 6 through 8 and again with δ as a parameter. Fig. 6 through 8 show that, within the range considered in this study, heat transfer enhancement increases with smaller values of ϵ , which is the case when the spacing between the holes, S_x , decreases and/or and hole's diameter, D, increases.

As far as the spacing between the holes, S_x , is concerned, it may be noted that as the spacing decreases, the number of holes per unit width increases. So, if having a hole in the fin increases the local heat transfer there, then increasing the number of holes (by decreasing the spacing between them) will increase the overall heat transfer. Moreover, it may be argued here that the flow coming out of the holes form vorticity that gets more vigorous when the spacing between the holes, S_x , becomes smaller. More vigorous vorticities better enhance other vorticities next to them resulting in better mixing that eventually improves heat transfer. Fig. 9

and 10 present two profiles for dimensionless vorticity, ω^* , distribution at the central section through the holes for the case $\delta = 0.15$ and $Gr = 106$ for two different values of ϵ , namely, 5 and 10. It can be readily seen from Fig. 9 and 10 that the two vorticity contours are quite similar but with different scales demonstrated by the higher maximum value of 7.6 of ω^* at the lower $\epsilon = 5$ compared to a maximum value of 6.7 at $\epsilon = 10$.

As for the hole diameter, D , it is established that as the diameter increases, buoyancy forces (that tend to push the flow through the holes against viscous forces) increase because the volume inside the hole increases whereas viscous forces (that tend to prevent flow from getting through) in each hole decrease because the characteristic length within which these forces act decreases leading to heat transfer enhancement. In addition, and viewed from a different perspective, if each hole is considered as a vertical "pipe" wherein heat is transferred naturally, each hole will have a local Grashof number similar to the overall Grashof number though with a different characteristic length where this length becomes the diameter of the hole rather than the length of the fin. This value of the local Grashof number is proportional to the hole or "pipe" diameter to the third power. Therefore, increasing the diameter will increase the local Grashof number and thus effect substantial increase in heat transfer in the hole as demonstrated above.

Careful examination of Fig. 5 and 8 indicates that, unlike the consistent trends reported on Fig. 3, 4, 6, and 7, things get a point where increasing the hole diameter in fact decreases heat transfer enhancement. At this point, let's introduce the parameter ΔA that expresses the change in the surface area of a fin with thickness t due to drilling a vertical hole with a diameter D through it. Then, ΔA is simply given by the following expression:

$$\Delta A = \pi Dt - 2 \frac{\pi D^2}{4} \quad (8)$$

Now, it may be readily shown that the plot of ΔA versus the hole diameter, D , is a parabola that starts from zero (at D equals zero), increases up to a maximum value where D is equal to the fin thickness, t , and decreases back to zero when D becomes twice the fin thickness. Once D becomes greater than $2t$, the curve continues to decrease in the negative direction meaning that drilling a hole (holes) results in a net reduction in the fin surface area compared to the solid counterpart. This demonstrates that there exists an optimum value for the hole diameter where the total surface area is maximum depending on the fin thickness, which is fixed at $0.1L$ in this study. This explains the deviation witnessed in Fig. 5 and 8 where heat transfer enhancement decreases with increasing the diameter of the holes beyond a given range.

4. Conclusion

Examining the findings of this study, it may be indicated that the introduction of circular perforations to the body of a rectangular fin under natural convection conditions may result in significant gains in heat transfer from the perforated fin relative to the solid counterpart and over a wide range of Grashof numbers. This is provided that the relevant geometrical parameters, most notably, hole diameter and spacing between holes is carefully controlled and maintained in the desirable ranges.

5. Acknowledgements.

The authors would like to express their gratitude to the Deanship of Scientific Research at King Faisal University, Al-Ahsa, Saudi Arabia, for funding this study. Thanks are also extended to Dr. Mutaz Al-Muhtaseb for the assistance he provided.

References

- [1] Incropera, F. and Dewitt, P.D. Introduction to Heat Transfer. 3rd ed. Chichester: John Wiley.
- [2] Bergles, A.E. The Implications and Challenges of Enhanced Heat Transfer for the Chemical Process Industries. Chem Eng Res Des, Vol. 79, 437–44 (2001).
- [3] Malekzadeh, P., Rahideh, H, and Karami, G. Optimization of Convective-Radiative Fins by Using Differential Quadrature, Element Method, Energy Conversion and Management, Vol. 47, 1505–14 (2006).
- [4] Arslanturk, C. and Ozguc, A.F. Optimization of a Central-Heating Radiator, Applied Energy, Vol. 83, 1190–1197 (2006).
- [5] Shaeri, M.R. and Yaghoubi, M.. Thermal Enhancement from Heat Sinks by Using Perforated Fins, Energy Conversion and Management, Vol. 50, 1264–1270 (2009).
- [6] Sahin, B. and Demir, A. Performance Analysis of a Heat Exchanger Having Perforated Square Fins, Applied Thermal Engineering, Vol. 28, 621–632 (2008).
- [7] Molki, M., and Hashemi-Esfahanian, A. Turbulent Convective Mass Transfer Downstream of a Perforated Baffle Blockage, Int. J. Heat Fluid Flow, Vol. 13 (2), 116–123 (1992).
- [8] AlEssa, A. H. and Al-Widyan, M.I., (2008). Enhancement of Natural Convection Heat Transfer from a Fin by Triangular Perforation of Bases Parallel and toward its Tip, Appl. Math. Mech. -Engl. Ed. (Shanghai University and Springer-Verlag), Vol. 29(8), 1033–1044 (2008).

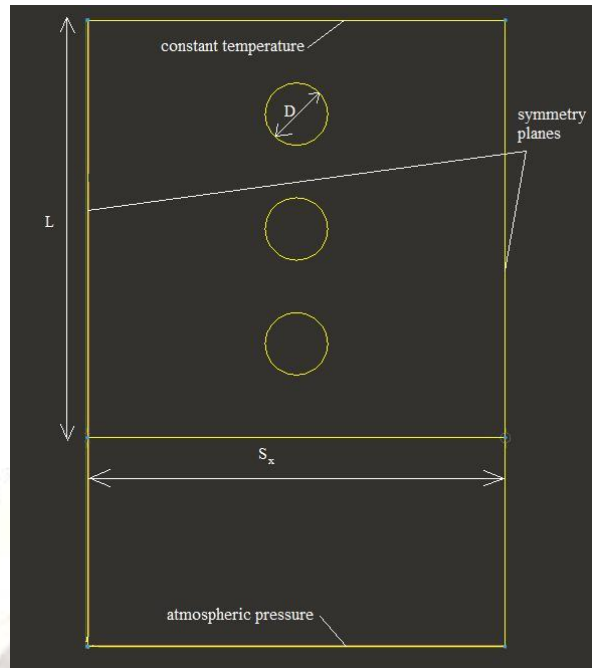


Figure 1. A schematic diagram of the fin considered in this study.

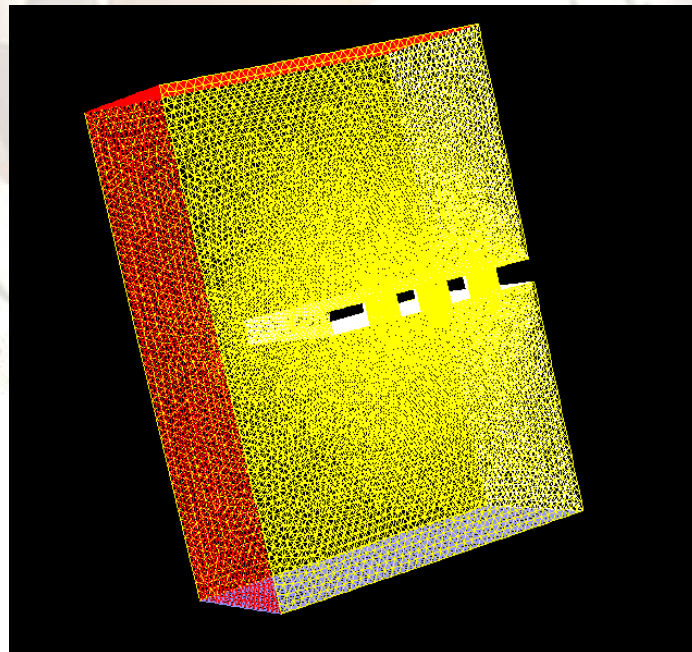


Figure 2. A sample of the mesh utilized for the perforated fin considered in this study.

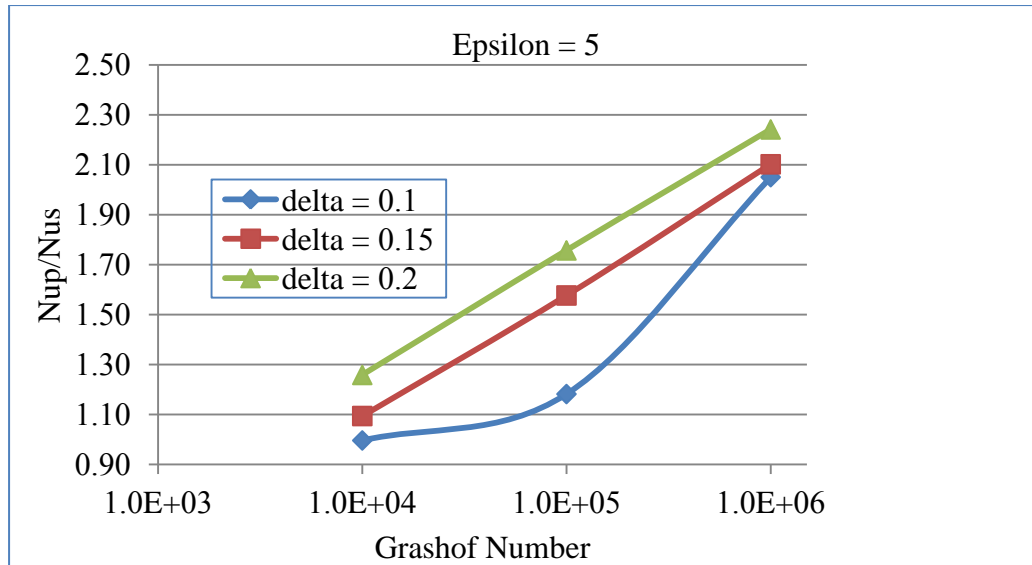


Figure 3. Heat transfer enhancement versus Gr with δ as a parameter for $\epsilon = 5$.

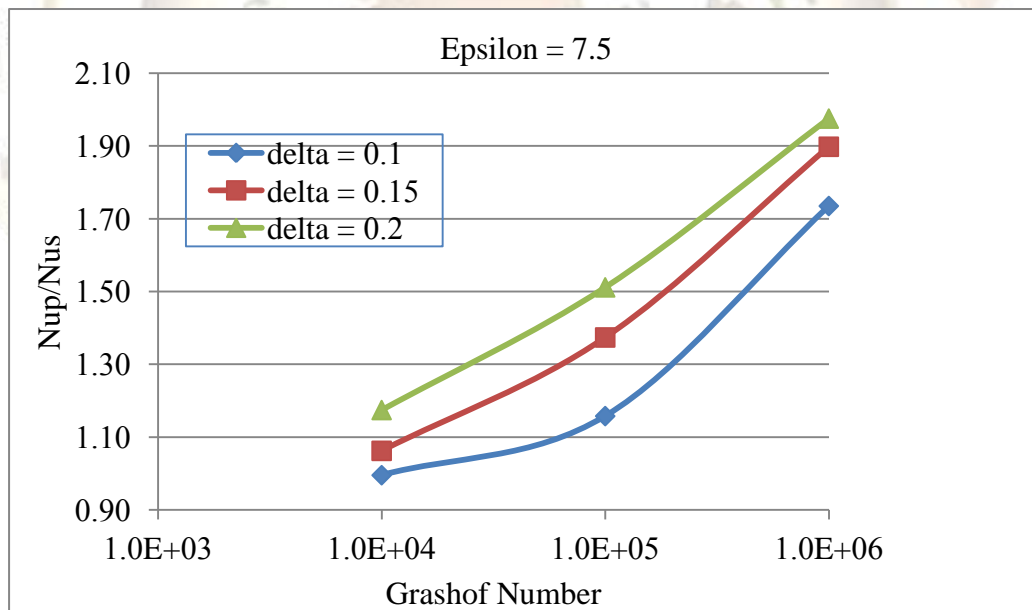


Figure 4. Heat transfer enhancement versus Gr with δ as a parameter for $\epsilon = 7.5$.

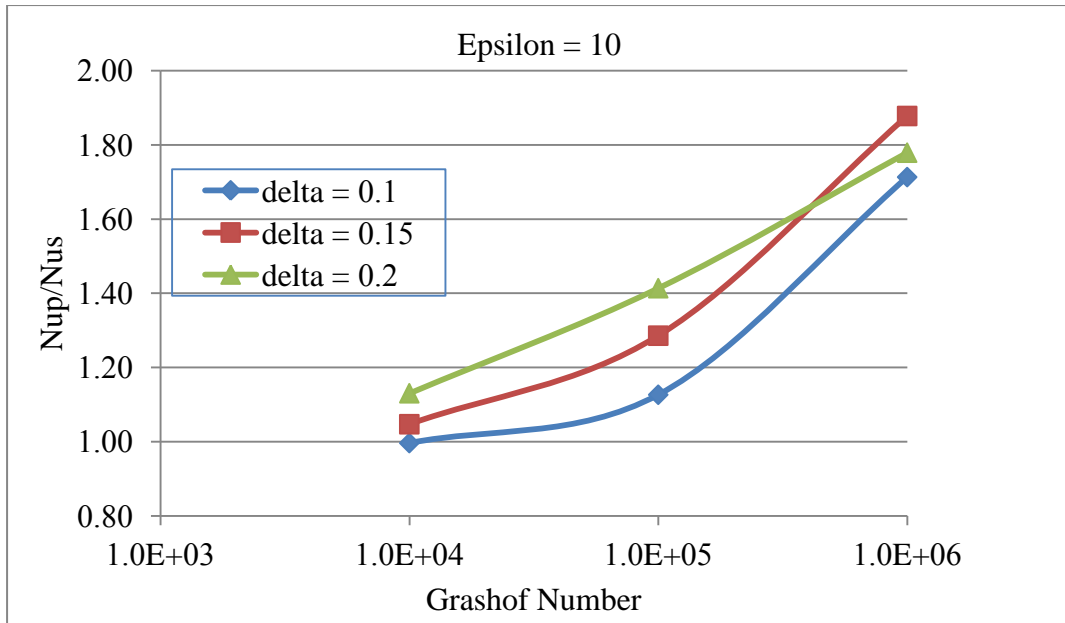


Figure 5. Heat transfer enhancement versus Gr with δ as a parameter for $\epsilon = 10$.

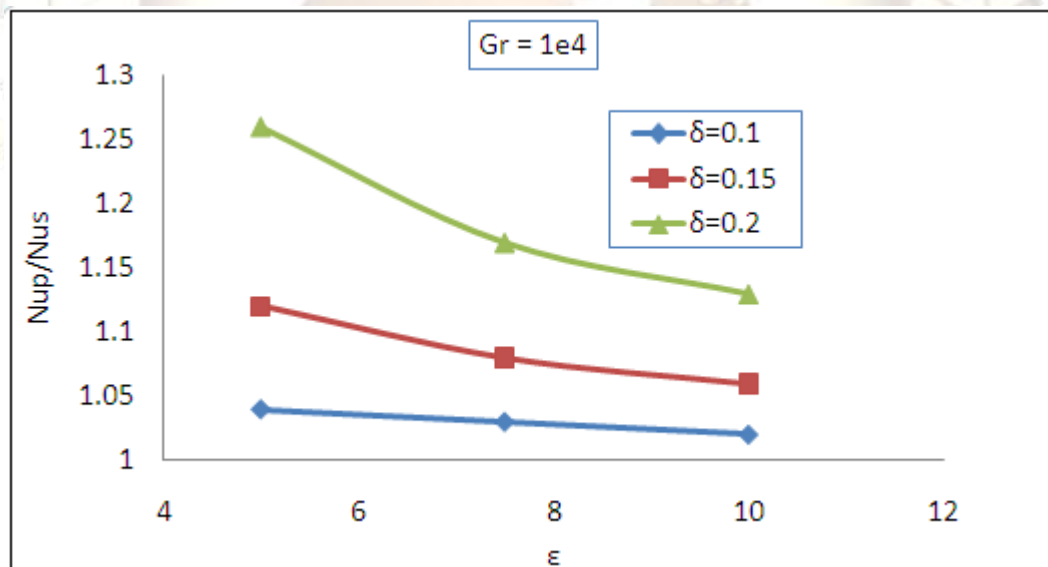


Figure 6. Heat transfer enhancement versus ϵ with δ as a parameter for $Gr = 10^4$.

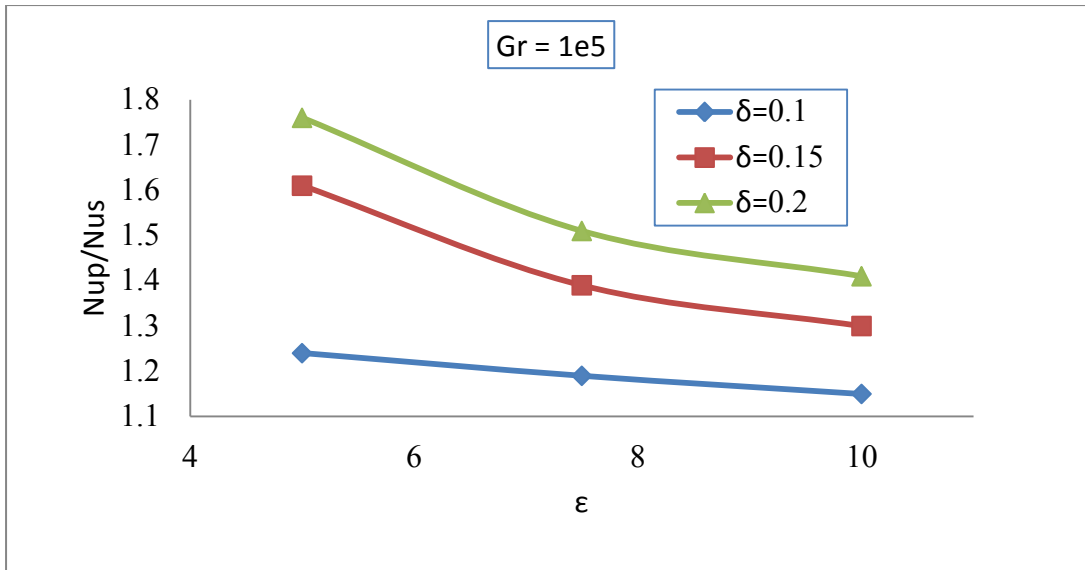


Figure 7. Heat transfer enhancement versus ϵ with δ as a parameter for $Gr = 10^5$.

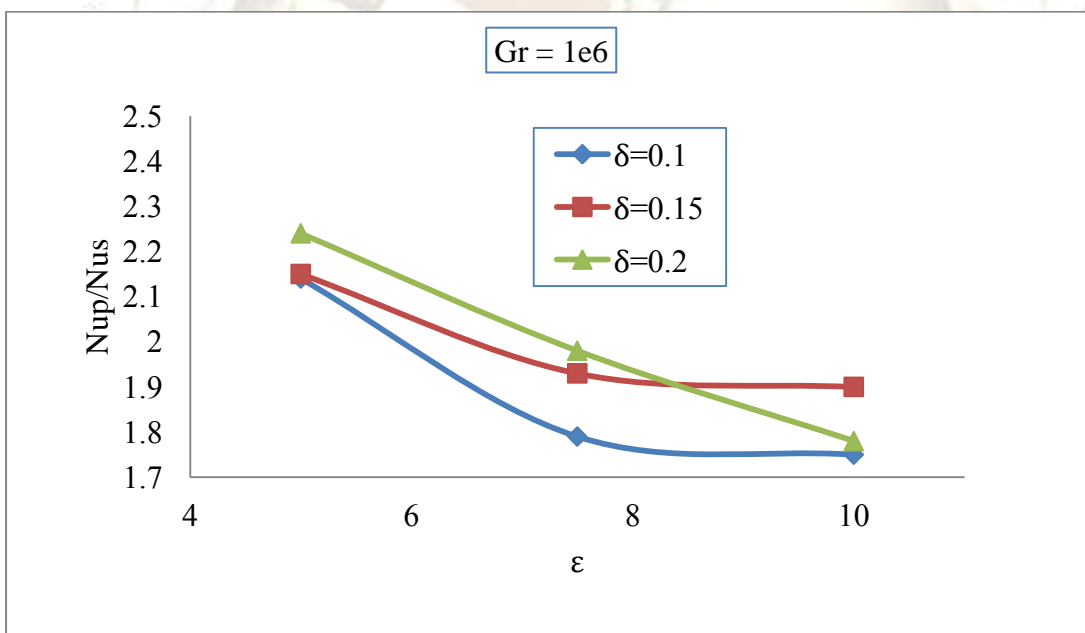


Figure 8. Heat transfer enhancement versus ϵ with δ as a parameter for $Gr = 10^6$.

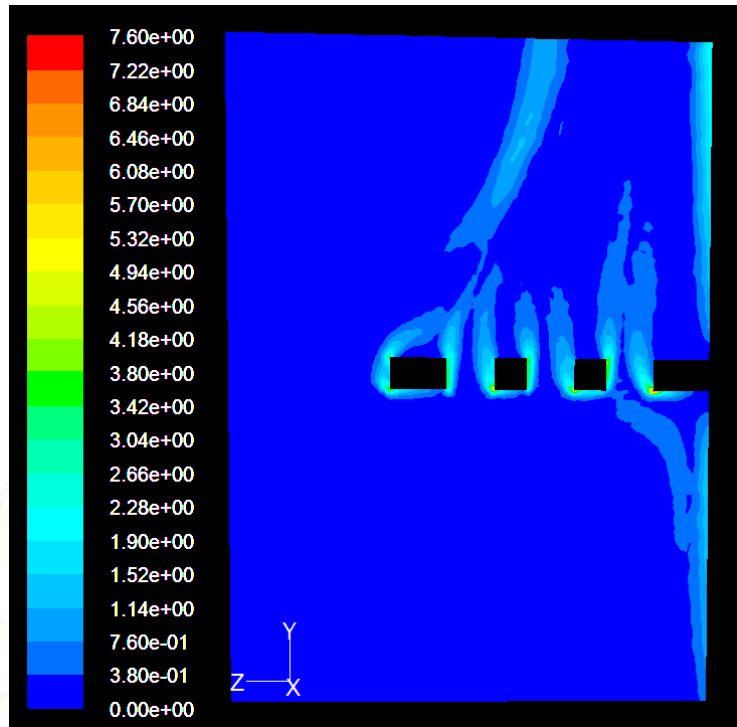


Figure 9. Dimensionless vorticity, ω^* , distribution profile (contour) at the central section through the holes for the case $\delta = 0.15$ and $Gr = 10^6$ ($\epsilon = 5$).

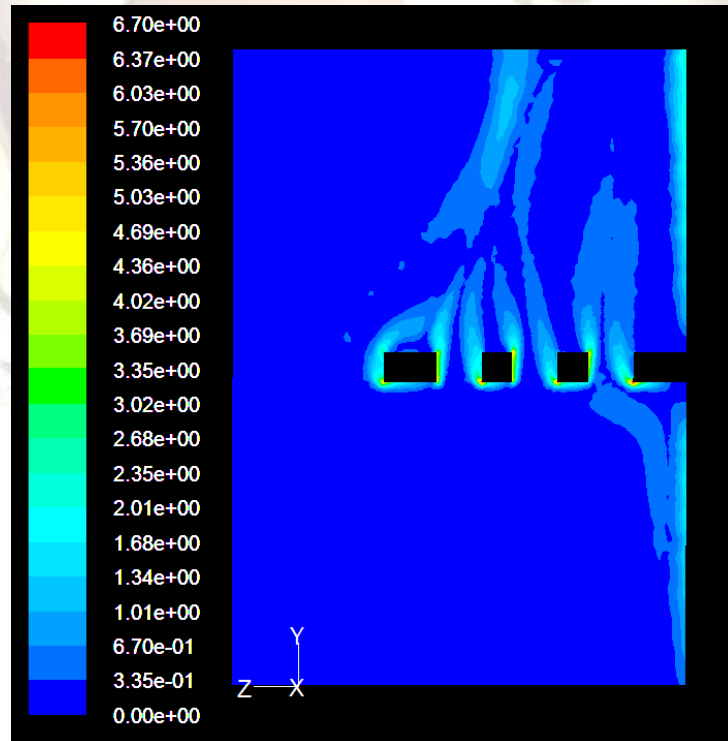


Figure 10. Figure 9. Dimensionless vorticity, ω^* , distribution profile (contour) at the central section through the holes for the case $\delta = 0.15$ and $Gr = 10^6$ ($\epsilon = 10$).